Small molecule-mediated inhibition of β-2-microglobulin-based amyloid fibril formation

Received for publication, December 23, 2016, and in revised form, May 2, 2017 Published, Papers in Press, May 3, 2017, DOI 10.1074/jbc.M116.774083

Tyler M. Marcinko, Jia Dong, Raquel LeBlanc, Kate V. Daborowski, and Richard W. Vachet[1]

From the Department of Chemistry, University of Massachusetts, Amherst, Massachusetts 01003

Edited by Paul E. Fraser

In dialysis patients, β-2 microglobulin (β2m) can aggregate and eventually form amyloid fibrils in a condition known as dialysis-related amyloidosis, which deleteriously affects joint and bone function. Recently, several small molecules have been identified as potential inhibitors of β2m amyloid formation *in vitro*. Here we investigated whether these molecules are more broadly applicable inhibitors of β2m amyloid formation by studying their effect on Cu(II)-induced β2m amyloid formation. Using a variety of biophysical techniques, we also examined their inhibitory mechanisms. We found that two molecules, doxycycline and rifamycin SV, can inhibit β2m amyloid formation *in vitro* by causing the formation of amorphous, redissolvable aggregates. Rather than interfering with β2m amyloid formation at the monomer stage, we found that doxycycline and rifamycin SV exert their effect by binding to oligomeric species both in solution and in gas phase. Their binding results in a diversion of the expected Cu(II)-induced progression of oligomers toward a heterogeneous collection of oligomers, including trimers and pentamers, that ultimately matures into amorphous aggregates. Using ion mobility mass spectrometry, we show that both inhibitors promote the compaction of the initially formed β2m dimer, which causes the formation of other off-pathway and amyloid-incompetent oligomers that are isomeric with amyloid-competent oligomers in some cases. Overall, our results suggest that doxycycline and rifamycin are general inhibitors of Cu(II)-induced β2m amyloid formation. Interestingly, the putative mechanism of their activity is different depending on how amyloid formation is initiated with β2m, which underscores the complexity of how these structures assemble *in vitro*.

Given the prevalence of amyloid diseases, such as Alzheimer's disease and Parkinson's disease, and type II diabetes, there has been great effort put toward developing small-molecule inhibitors of amyloid formation (1, 2). To properly employ such therapeutics, it is important to understand how potential candidates affect the amyloid assembly process. There are several potential strategies for disrupting amyloid formation, including stabilizing the native state of the protein, destabilizing or kinetically trapping early soluble oligomers, and/or promoting off-pathway aggregation.

In this study, we explore how several small molecules influence the amyloid fibril formation pathway of the protein β-2 microglobulin (β2m),[2] which is the protein implicated in dialysis-related amyloidosis (3, 4). β2m is a 99-residue protein composed of seven β strands arranged in an anti-parallel β sandwich motif held together by a lone disulfide bond (5). Although it is normally a structural component of the class I major histocompatibility complex, elevated serum concentrations of β2m, as a result of long-term dialysis, result in deposition of β2m amyloid fibrils in patient joints, ultimately resulting in joint destruction (6). β2m amyloid fibril formation has been studied extensively *in vitro*, and several conditions can convert the protein from soluble to insoluble amyloids, including low pH conditions, trifluoroethanol (TFE), thermal denaturation, partial denaturation with lysophospholipids, deletion of the first six amino acids, and incubation with catalytic amounts of Cu(II) (7–20).

There has also been some preliminary work on identifying and studying potential inhibitors of β2m amyloid formation. Small molecules capable of binding to β2m and, in some cases, inhibiting its amyloid formation, have been studied using surface plasmon resonance, capillary electrophoresis, electrospray ionization MS (ESI-MS), ion mobility spectrometry, and computational simulations (21–25). A few small molecules have been found to inhibit β2m amyloid formation when initiated by acid or TFE addition (23, 24). These studies suggest that the effective inhibitors preferentially bind to partially or natively structured β2m and exert their inhibitory effect on the monomeric form of the protein, causing the formation of spherical instead of fibrillar aggregates. The impact of these molecules on the Cu(II)-catalyzed amyloid assembly pathway of β2m, however, has not been reported. Such studies represent an opportunity to determine whether these molecules are more broadly capable of inhibiting β2m amyloid formation, especially under physiologically relevant pH and ionic strengths (*i.e.* pH 7.4, 150 mM ionic strength). As reported previously by our group and others, Cu(II) binding to β2m causes several structural changes that allow β2m to oligomerize and eventually form amyloid fibrils. Oligomerization has been shown to proceed through discrete stages (*i.e.* formation of dimers, tetramers, and hexam-

This work was supported by National Institutes of Health Grant R01 GM 075092. The authors declare that they have no conflicts of interest with the contents of this article. The content is solely the responsibility of the authors and does not necessarily represent the official views of the National Institutes of Health.
This article contains supplemental Figs. S1–S5.

[1] To whom correspondence should be addressed. Tel.: 413-545-2733; E-mail: rwvachet@chem.umass.edu.

[2] The abbreviations used are: β2m, β-2-microglobulin; TFE, trifluoroethanol; ESI, electrospray ionization; Dox, doxycycline; Rif, rifamycin SV; Sur, suramin; TEM, transmission electron microscopy; SEC, size exclusion chromatography; CCS, collisional cross-section.

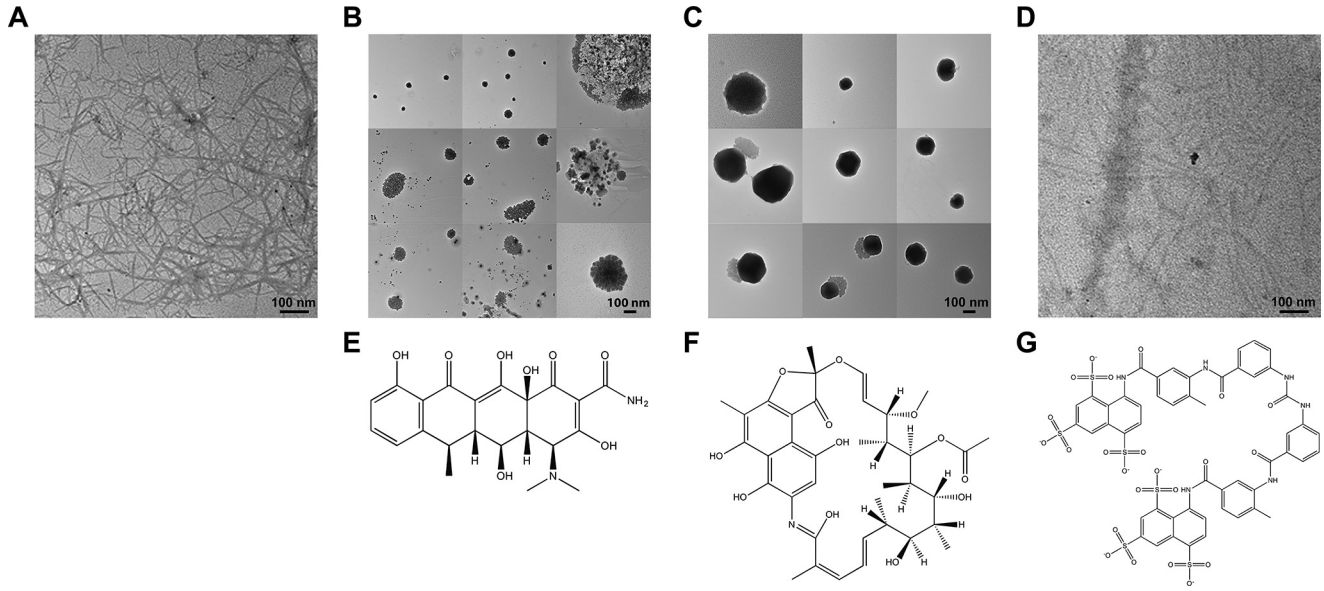

Figure 1. The addition of doxycycline or rifamycin alters insoluble aggregate morphology under Cu(II)-catalyzed β2m amyloid formation conditions after 14 days of incubation at 37 °C. Samples contained 100 μM β2m, 200 μM Cu(II), and the corresponding small molecule (100 μM). *A–D*, TEM images at ×25,000 magnification of the control (*A*), doxycycline (*B*), rifamycin (*C*), and suramin (*D*) samples. *E–G*, structures of Dox (*E*), Rif (*F*), and Sur (*G*).

ers) that are necessary for amyloid formation *in vitro* (12–20). Moreover, studying the effect of small molecules on the Cu(II)-catalyzed pathway provides an opportunity to investigate commonalities in the inhibition modes between different amyloid-forming conditions.

We explore in this work three small molecules, doxycycline (Dox), rifamycin SV (Rif), and suramin (Sur), that are known to bind β2m and/or influence its amyloid assembly when initiated by acid or TFE. To more deeply understand how these molecules affect Cu(II)-induced β2m amyloid formation, we use a variety of biophysical techniques to study perturbations in the assembly of β2m oligomers and amyloid aggregates. We find that Dox and Rif inhibit amyloid formation by diverting β2m oligomers along a different pathway that leads to amorphous aggregates. Moreover, using ESI-MS and ion mobility spectrometry, we find that the inhibitors exert their influence by specifically perturbing the structures of β2m dimers and tetramers. Overall, our study suggests that certain small molecules can generally inhibit β2m amyloid formation, but the mechanism is likely different depending on how amyloid formation is initiated.

Results

To test the ability of small molecules to inhibit the amyloid assembly process of β2m, we assessed the morphology of any resulting insoluble aggregates using TEM (Fig. 1). Following centrifugation, insoluble material was present in all sample tubes after 14 days of incubation. Amyloid fibrils were observed in both the control and the Sur-treated samples. Some amorphous aggregates were also observed in the TEM images of the Sur sample. In addition, a smaller insoluble pellet was observed in the Sur sample compared with the control, suggesting perhaps that Sur either slows the fibrillization process or only partially affects it. The dimensions and morphology of the fibrils observed in the control and Sur samples were consistent with amyloid fibrils published previously (15, 16). Thioflavin T fluorescence experiments were also attempted, but the presence of the inhibitor molecules was found to interfere with the spectral properties of thioflavin T, therefore compromising the results of the assay. Such interferences were also observed for similar compounds by other groups (23, 26).

In the Dox- and Rif-treated samples, the morphology of the insoluble aggregates was drastically different. Rather than elongated fibrils, we observed dense amorphous particles that appeared to be evenly distributed with no evidence of fibrillar structures. When comparing Dox-treated aggregates with Rif-treated aggregates, the Dox-treated aggregates had a granular quality that either existed as discrete particles with diameters of ~5–10 nm or as part of larger aggregated clusters that ranged in size from about 200–500 nm. In contrast, the Rif-treated aggregates had larger amorphous structures with diameters that ranged from about 100–300 nm. In many cases, after resuspension of the insoluble material in 2% SDS and incubation at 37 °C for 24 h, the Dox- and Rif-treated samples were found to be completely redissolvable.

We then assessed the impact of the small molecules on the oligomerization process that precedes fibril formation (Fig. 2, *A–D*). Over the course of 6 days, peaks corresponding to dimers, tetramers, and hexamers were measured for both the control and Sur-treated samples. The soluble oligomer profiles for the control and Sur-treated samples were consistent with previous work from our group (15, 16). The oligomeric species in the Sur samples tended to be less abundant than the control samples at the same time periods, which is consistent with Sur slowing but not inhibiting amyloid formation.

The presence of Dox or Rif changed the oligomerization profile. Rather than the formation of discrete even-numbered oligomers, peaks corresponding to a trimer were measured for both molecules. More interestingly, a large, broadly eluting peak was measured at higher molecular weights for both inhibitors. According to the calibration curve, species eluting during this

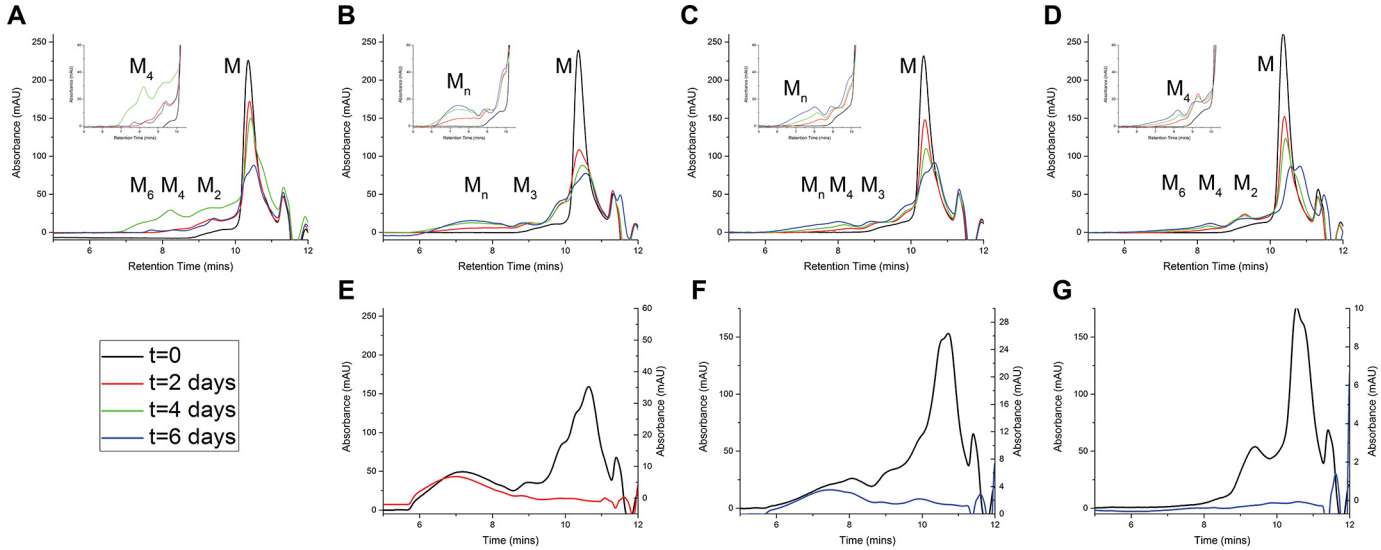

Figure 2. Doxycycline and rifamycin alter the soluble Cu(II) oligomerization profile and remain bound to oligomers in solution phase. *A–D*, SEC results over the course of 6 days of incubation at 37 °C for control (*A*), Dox (*B*), Rif (*C*), and Sur (*D*). *Insets*, expanded views of the oligomer elution region. *E–G*, SEC-HPLC results after 6 days of incubation for Dox (*E*), Rif (*F*), and Sur (*G*). In *E–G*, the *black traces* correspond to the variable wavelength detector set to 214 nm, whereas the *colored traces* corresponds to 350 nm (*red*) or 315 nm (*blue*). Samples contained 100 μM β2m, 200 μM Cu(II), and the corresponding small molecule (100 μM) in *A–D* and 150 μM β2m, 300 μM Cu(II), and the corresponding small molecule (150 μM) in *E–G*.

range had estimated molecular weights ranging from a pentamer to an octamer.

Furthermore, there is a prominent tetrameric species that was observed in the Rif-containing sample. The oligomeric profiles observed with Dox and Rif were in contrast to the control and Sur-treated samples and consistent with the altered aggregate morphologies observed with these two inhibitors. We also performed an experiment in which inhibitor addition was delayed until dimers (2 days) or tetramers (4 days) were formed. For both Dox and Rif, the normal oligomer population was converted to an oligomer profile similar to the ones measured when the inhibitor was present from the start of the incubation (supplemental Fig. S1).

Because each of the small molecules studied here absorbs at higher wavelengths than the protein, we could also separately detect when the small molecules were eluting and determine with which protein species they were associated. Overlays of the chromatograms showing the protein absorption and the small molecule absorptions indicate that both Dox and Rif elute primarily with the oligomeric species, suggesting preferential interactions with the β2m oligomers, whereas Sur does not (Fig. 2, *E–G*). Blank solutions of each inhibitor dissolved in water at identical concentrations were also injected, and they were found to elute after the monomer peak (supplemental Fig. S2), confirming that the small molecules only elute earlier because of interactions with β2m oligomers. Expanded chromatograms displaying the entire elution profile can also be found in supplemental Fig. S3, showing that Sur primarily elutes after the protein, indicating that it does not interact strongly with the monomer or any of the oligomers. Interestingly, after 14 days, when the precipitates are formed, we found that all small molecules (*i.e.* Dox, Rif, and Sur) were free in solution rather than associated with the protein aggregates (data not shown).

To further investigate the identities of the oligomers that are present in the inhibitor-containing solutions (*i.e.* Dox and Rif), we employed native electrospray ionization mass spectrometry (*e.g.* Fig. 3). Peak assignments were based on charge-state deconvolutions and collision-induced dissociation data for each ionic species (*e.g.* supplemental Fig. S4). For the control sample, even-numbered oligomers, but not odd-numbered ones, were observed at incubation times of up to 6 days, which is consistent with both the SEC data (Fig. 2) and previous results from our group (15, 16). In contrast to the control samples, the presence of Dox or Rif altered the oligomer profile by forming trimers and pentamers in addition to even-numbered oligomers. Furthermore, peaks corresponding to inhibitor-bound species were observed for both Dox and Rif for several oligomeric charge states. Many of these oligomer-inhibitor complexes can be readily resolved in the mass spectra from the Rif samples, but in the Dox samples it was difficult to confirm the inhibitor-bound species in some cases. Collision-induced dissociation of the suspected inhibitor-bound oligomers, however, confirmed that the inhibitors were bound to the oligomers, as a second charge-state distribution of inhibitor-adducted monomer ions was clearly observed (Fig. 4).

The β2m oligomers and their inhibitor complexes from the various samples were also monitored by ion mobility mass spectrometry to analyze for the presence of conformational isomers (conformers) as a way to assess the structural effects of the inhibitors on β2m and its oligomers. Numerous previous studies have demonstrated that ion mobility can provide useful insights into the stoichiometry and architecture of non-covalent complexes as well as the presence of conformational isomers (27–29). Fig. 5 illustrates the key differences that are observed between β2m oligomers formed in the absence and presence of the inhibitors. The monomers, dimers, and tetramers of both control and inhibitor-containing samples were compared, as these β2m species are common to both sets of samples. For the monomer ions, only a single conformation was observed for the control or inhibitor-containing species,

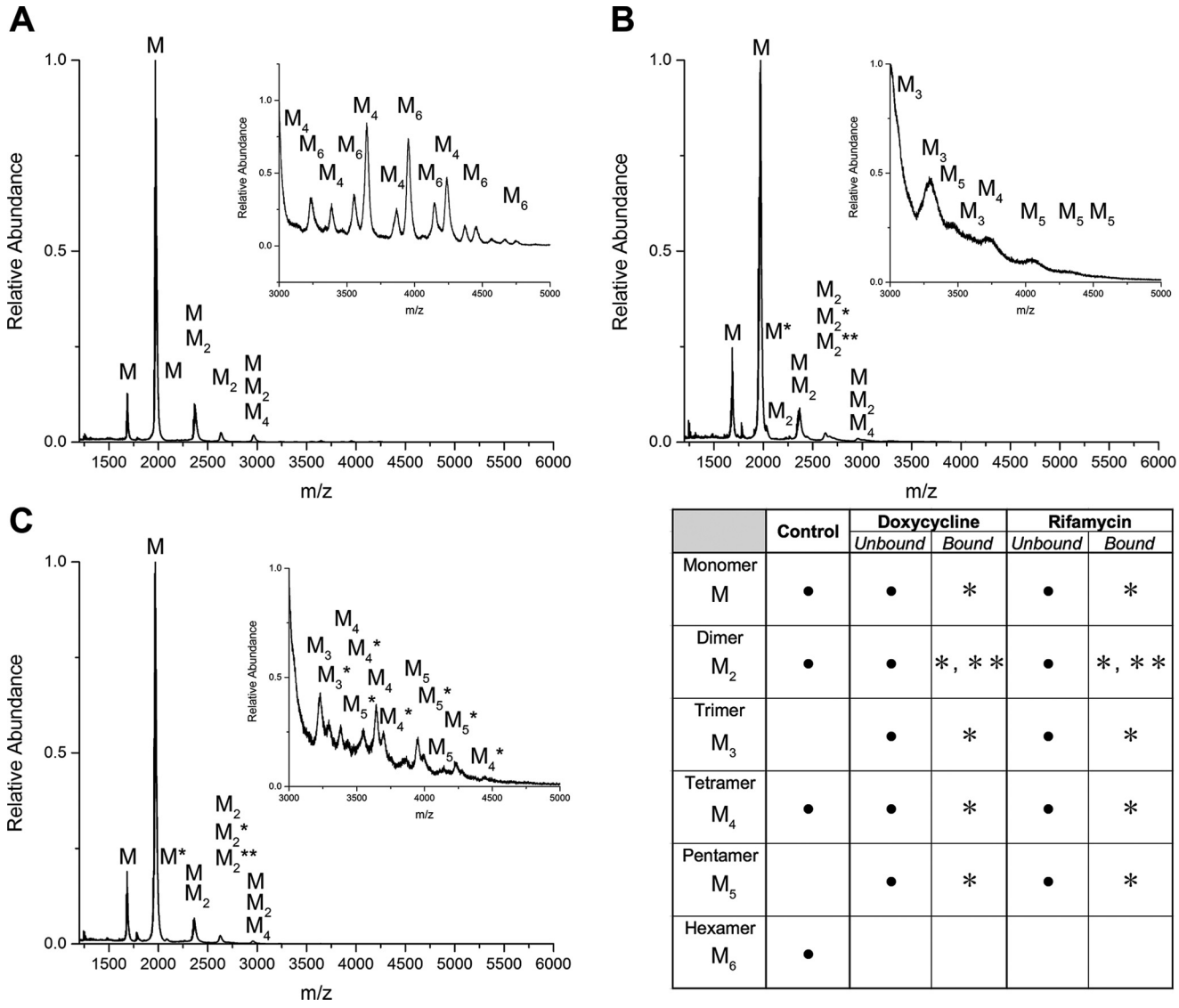

	Control	Doxycycline		Rifamycin	
		Unbound	*Bound*	*Unbound*	*Bound*
Monomer M	●	●	*	●	*
Dimer M_2	●	●	*, **	●	*, **
Trimer M_3		●	*	●	*
Tetramer M_4	●	●	*	●	*
Pentamer M_5		●	*	●	*
Hexamer M_6	●				

Figure 3. Nano-ESI-IMS-MS reveals identities of soluble oligomeric species. *A–C*, native spray data after 6 days of incubation at 37 °C for control (*A*), Dox (*B*), and Rif (*C*). Samples were desalted into 100 mM ammonium acetate prior to analysis. The samples contained 100 μM β2m, 200 μM Cu(II), and the corresponding small molecule (100 μM). Sample concentration was 10 μM after desalting. Data for all samples were collected under identical instrumental conditions. In the associated table, ● signifies the confirmation of the presence of an oligomer, whereas an *asterisk* denotes the presence of a small molecule-bound adduct.

whether monitoring the ions without (Fig. 5*A*) or with (Fig. 5*D*) the inhibitor bound. The inhibitor-bound complex ions for the predominant conformers (Fig. 5, *C–F*) showed small increases in collision cross-section (CCS) values compared with the control samples, but these changes were insignificant in many cases.

When the inhibitors were present, though, differences in the number of conformers and the CCS values of the new conformers were apparent for the dimer and tetramer. For the dimer, a more compact conformer was present in both the inhibitor-free (Fig. 5*B*) and inhibitor-bound (Fig. 5*E*) complex ions. The compact dimer is much more abundant in the dimer-inhibitor complex ions (Fig. 5*E*), especially for the Rif samples, suggesting that this dimer conformer was part of the effect of Rif on the aggregation process. A more striking difference was seen in the arrival time distributions of the tetramer. The control sample indicated the presence of three conformers, including an expanded conformer with a CCS value of ~3600 Å^2 (Fig. 5*C*). The more expanded conformer was absent in the inhibitor-containing samples (Fig. 5, *C* and *F*), indicating perhaps that the inhibitors influenced the aggregation process by preventing the formation of this more expanded structure. There was also a small increase in the CCS value of the main conformer observed when Dox and Rif were present in the solution.

Discussion

This study represents the first time that the effect of small-molecule inhibitors on Cu(II)-catalyzed β2m amyloid formation has been investigated. The small molecules studied here were chosen because they are known to bind to β2m and/or inhibit β2m amyloid formation that is initiated by other means (*e.g.* with acid or 20% trifluoroethanol) (21–25). In contrast to these previous studies, our experiments were conducted under physiologically relevant conditions (*i.e.* pH 7.4 and an ionic strength of 150 mM). The fact that both Dox and Rif prevented amyloid formation that was initiated by Cu(II) *and* by other

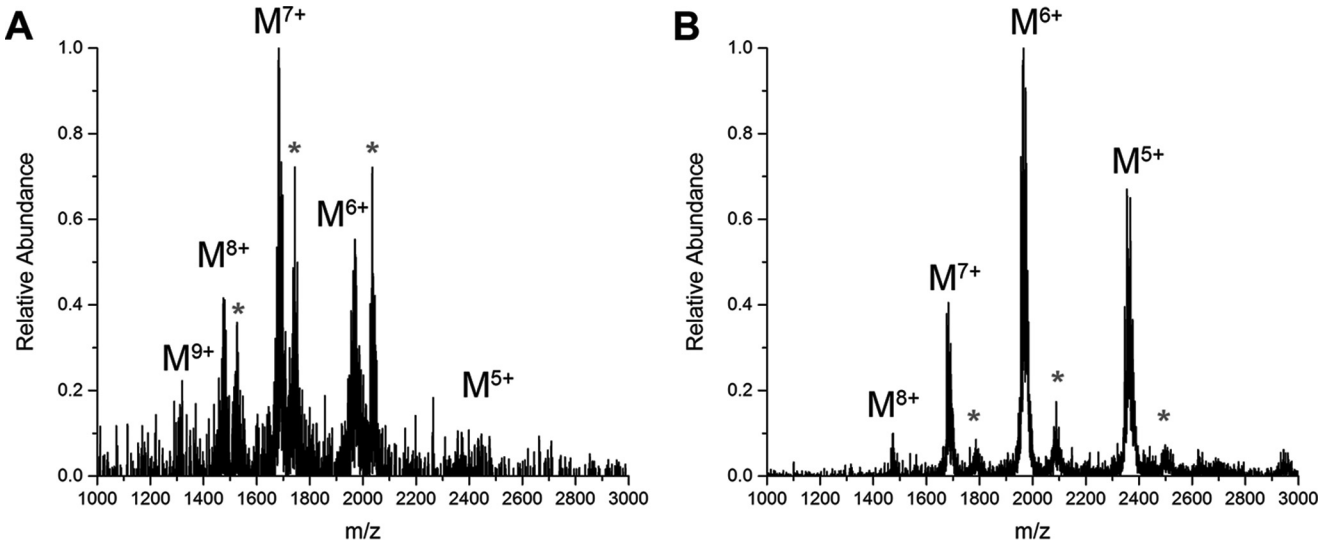

Figure 4. Collision-induced dissociation of oligomers confirms that Dox and Rif are bound in gas phase. Shown are spectra of an activated monomer and a small-molecule adduct (*asterisks*) dissociated from a 13+ tetramer for Dox (*A*) and Rif (*B*).

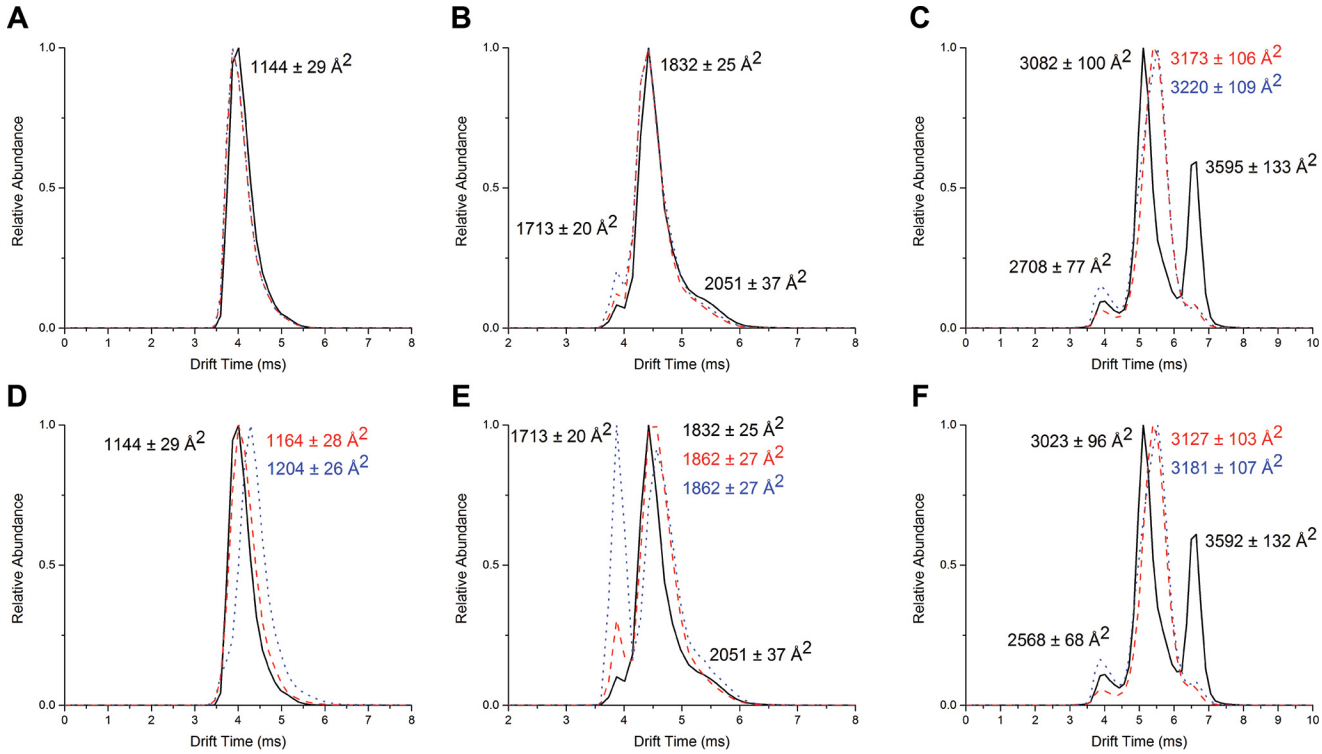

Figure 5. Arrival time distributions and CCS values reveal conformational and structural differences in oligomer populations. CCS values were estimated using a calibration curve and calculations as described under "Experimental procedures." *A–C*, unbound comparisons of the 6+ monomer (*A*), 9+ dimer (*B*), and 14+ unbound tetramer (*C*). *D—F*, comparisons of the unbound control and the inhibitor-bound versions of the 6+ monomer (*D*), 9+ dimer (*E*), and 14+ tetramer (*F*). The control is shown as *black lines*, Dox as *red dashed lines*, and Rif as *blue dotted lines*.

means further suggests the promise of these molecules as inhibitors of β2m amyloid formation. Our results also suggest some commonalities between the Cu(II)-induced amyloid pathway and the amyloid pathways induced by acid or TFE. Moreover, the fact that Sur did not prevent amyloid formation further connects the different modes of initiating β2m amyloid formation, as this molecule behaved similarly under amyloid-inducing conditions involving TFE (22).

The apparent commonalities in how Dox and Rif prevent β2m amyloid formation that is initiated by different means motivated our attempts to understand the molecular basis of this inhibition, although it appears that these molecules influence the pathways at different points. Previous work with TFE suggested that Dox inhibits β2m self-association while stabilizing native-like structures (24). Under acidic conditions, Rif inhibits fibrillization via binding to specific conformations of the monomer and dimer and is capable of disassembling oligomers by favoring inhibitor-bound monomers (23). In contrast, our results indicate that the inhibitors interact more favorably with larger oligomeric species (≥ dimer), thus diverting the

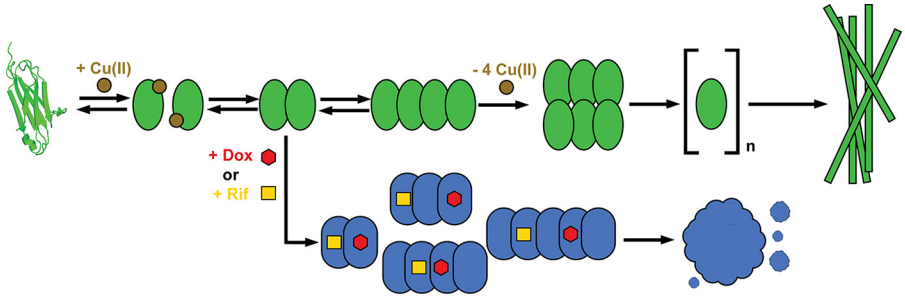

Figure 6. Dox and Rif alter the amyloid assembly pathway, yielding distinct soluble and insoluble oligomeric structures.

amyloid-competent oligomerization pathway (*e.g.* Fig. 2) toward redissolvable aggregates with non-fibrillar morphologies (Fig. 1). Dox and Rif divert the normal Cu(II)-induced oligomer assembly process, whether present at the beginning of the incubation or when added after the oligomers are already present (Fig. 2, *A–D*, and supplemental Fig. S1), so that more than just even-ordered oligomers are formed. The loss of an ordered oligomer assembly process might explain why amorphous aggregates are formed in the presence of the inhibitors.

The increased oligomer heterogeneity observed when the inhibitors are present indicates that these small molecules change the structures of the preamyloid oligomers and/or perturb the specific interactions of the preamyloid oligomers that enable them to progress to a fibrillar morphology. The structural and oligomeric changes are presumably enforced by the preferential binding of Dox and Rif to the higher-order oligomers, as revealed by the SEC data shown in Fig. 2, *E* and *F*. The inhibitors, however, are eventually released upon formation of the amorphous aggregates, as indicated by their presence in the isolated supernatant. The exact molecular-level details of the structural changes are not known, but some insight into the structural differences between the on- and off-pathway oligomers was obtained using ion mobility and MS. Ion mobility has been increasingly used to characterize protein complexes, as evidence shows that proteins maintain aspects of their solution-phase structures during the ion mobility measurements (30–32). Moreover, in many cases, CCS values obtained from ion mobility measurements are found to correlate to solution-phase conformations (33–37). In the current context, ion mobility reveals the presence of isomeric protein oligomers (Fig. 5). The appearance of a more compact conformer for the dimer when the inhibitors are present suggests that the inhibitors exert their effect at this stage of the aggregation process, especially given the fact that CCS values for the inhibitor-bound and inhibitor-free monomers are essentially unchanged (Fig. 5*E*).

Compaction of the dimer might cause key residues that are important for tetramer assembly to be inaccessible, thereby preventing proper tetramer assembly. Furthermore, the structural remodeling the inhibitors exert on the dimer appears to be responsible for altering the oligomerization pathway so that trimers and pentamers are formed. In previous work, we established a model of the preamyloid dimer based on covalent labeling/MS data and molecular dynamics simulations. This dimer, which has similar structural features as one of the dimer units in the crystallographic hexamer formed by the non-amyloidogenic H13F mutant (PDB code 3CIQ), is calculated to have a CCS of 1831 Å^2, which is in excellent agreement with the experimentally determined value of 1830 ± 30 Å^2 (Fig. 5*B*) (17). The more compact dimer, which is formed in the presence of the inhibitors (Fig. 5*E*), has a CCS value that is 120 Å^2 smaller, representing a 6.6% decrease. This compaction would correspond to roughly 13 residues in the dimer, which is probably an extensive enough change to disrupt key residues involved in the amyloid-competent tetramer.

Compaction of the dimer in the presence of Dox and Rif not only indicates that these molecules exert their effect at this stage of the aggregation process, but it may also explain the dramatic difference in the tetramer conformers when the inhibitors are present. The most notable change is the complete disappearance of the elongated conformer with a CCS value of 3600 ± 100 Å^2 (Fig. 5, *C* and *F*). In previous work, we found that two preamyloid tetramers are formed upon incubation with Cu(II), one with Cu(II) bound and the other with Cu(II) absent, and formation of the Cu(II)-free tetramer is necessary for eventual amyloid formation (15). Based on this previous work, it is reasonable to conclude that the elongated tetramer measured here is the Cu(II)-free tetramer and that its disappearance in the presence of the inhibitors may explain why amyloid formation is not possible in the presence of these molecules. A more open conformation might be expected for the Cu(II)-free tetramer as residues previously constrained by binding to Cu(II) are released. Interestingly, we previously reported a structural model of the tetramer based on covalent labeling/MS measurements and molecular dynamics simulations (18). The calculated CCS value of this model is 2952 Å^2, which is remarkably close to the measured CCS value (*i.e.* 3000 ± 100 Å^2) of the predominant conformer, suggesting that our previous structural model is of the Cu(II)-bound tetramer.

Overall, our results indicate that Dox and Rif perturb the Cu(II)-induced amyloid process by diverting preamyloid aggregation along a pathway that is less ordered in terms of oligomer sizes and more amorphous in terms of the final insoluble material (Fig. 6). The process begins with compaction of the dimer that presumably enables the formation of trimers instead of the tetramers that are normally observed on the amyloid pathway. The inhibitors also appear to prevent the formation of an elongated tetramer, which may be the Cu(II)-free tetramer that is required to eventually form an amyloid-competent nucleus (15). Interestingly, tetracyclines like Dox are known to bind divalent metals like Cu(II), suggesting that they might influence

Cu(II)-β2m interactions (38, 39). The affinities of tetracyclines for Cu(II), however, are typically lower than the affinity of β2m for Cu(II) (38). Moreover, Dox is known to precipitate readily upon binding to Cu(II) in aqueous solutions (39). Because the only precipitation we observe is the formation of amorphous protein aggregates after 2+ weeks of incubation in the presence of Dox, we conclude that β2m-Cu(II) interactions remain mostly unaffected. The affinity of β2m for Cu(II) changes in the presence of Dox (K_d = 1.2 μM without Dox and 30 μM with Dox) (see supplemental Fig. S5), yet the Cu(II) concentrations used in this study are such that the majority of β2m is bound to Cu(II). Moreover, we have preliminary results (data not shown) that indicate that Dox binds to a site distant from the Cu(II) binding site, which likely explains the increase in K_d value observed in the presence of this small molecule. From these considerations, we conclude that the observed effect of Dox is attributed to its interaction with the protein oligomers, as indicated by the ion mobility mass spectrometry data.

The observation that the inhibitors influence the β2m amyloid formation process at the oligomer stage rather than at the monomer stage is somewhat unexpected. Work on other amyloid systems, including amyloid β and transthyretin, has also shown that small molecules can inhibit amyloid formation by working on oligomeric species rather than at the monomeric level, but our work is the first evidence of this occurring with β2m (40–42). Although amyloid inhibition is a desirable outcome in general, generating off-pathway aggregates during the process could lead to other undesired consequences, such as unexpected cellular toxicity (43–47). Thus, studies like the ones described here, which seek to gain insight into the mechanism of inhibition, are important for understanding possible side effects of amyloid inhibition.

Dox and Rif inhibit the amyloid fibril formation of β2m by causing the establishment of an alternative oligomerization pathway that ultimately produces amorphous, redissolvable aggregates. Rather than interfering with the amyloid pathway at the monomer stage, these molecules initially exert their influence on the dimer, causing compaction of this oligomer, which leads to the formation of larger oligomers that are incapable of forming amyloid fibrils. Dox and Rif also prevent the formation of an amyloid-competent tetramer that was found previously to be an essential step along the Cu(II)-induced amyloid pathway. These inhibitors remain bound to the early oligomers that populate the alternate aggregation pathway, suggesting that they reinforce the structural changes caused by their binding; however, the molecules are released upon formation of the larger amorphous precipitates that are eventually formed. Overall, the results from this study not only describe molecules that can inhibit β2m amyloid formation but also reveal that inhibitors can work by diverting, rather than preventing, the aggregation pathway of β2m by causing somewhat subtle structural changes to preamyloid oligomers. Moreover, this study demonstrates the value of native ESI-MS and ion mobility for revealing the β2m oligomer structural changes that are associated with amyloid inhibition.

Experimental procedures

Materials

Human full-length β2m (catalog no. 126-11) was purchased from Lee Biosolutions (Maryland Heights, MO). All chemicals and proteins, unless otherwise noted, were purchased from Sigma-Aldrich (St. Louis, MO). Solid phosphotungstic acid (catalog no. 19500) was purchased from Electron Microscopy Services (Hatfield, PA).

Formation of β2m oligomers and amyloid fibrils

For induction of β2m amyloid formation, a 1:2 molar ratio of protein to Cu(II) was used in a solution of 25 mM MOPS, 150 mM potassium acetate, and 500 mM urea at pH 7.4 as described in our previous work (15–18). Protein concentrations ranged from 50–150 μM. Where applicable, Dox, Rif, or Sur were added to the above incubation mixture at a molar ratio of 1:2:1 protein:copper:small molecule. A range of Dox, Rif, and Sur concentrations was explored, but a 1:1 ratio of protein:small molecule was found to be effective in all cases. Samples were incubated at 37 °C for varying time points (≤ 14 days) and then analyzed using several different techniques.

Size exclusion chromatography (SEC)

An HP Agilent 1100 series HPLC system fitted with a SuperSW2000 (catalog no. 18674) SEC column from Tosoh Bioscience, LLC (Tokyo, Japan) was used for all chromatographic analyses. The mobile phase consisted of 150 mM ammonium acetate (pH 6.9) and was used at a flow rate of 0.35 ml/min. For detection of proteins and β2m oligomers, the detector was set to 214 nm. For the detection of small molecules, the detector was set to 350 nm for Dox and 315 nm for Rif and Sur. A calibration standard mixture of bovine serum albumin, ovalbumin, carbonic anhydrase, and β2m was used to estimate molecular weights from SEC elution times.

ESI Ion Mobility MS

A Waters Synapt G2-Si quadrupole TOF mass spectrometer (Milford, MA) equipped with a nanospray source was used to collect all mass spectral data. The electrospray capillary voltage was set to 1.0 kV, the source temperature was set to 30 °C, and the source offset and sampling cone were set at 20 V. All other source and instrumental parameters were optimized to maximize protein complex ion signals. Electrospray capillaries were prepared in-house using established protocols by sputter-coating gold onto pulled borosilicate thin-wall capillaries (catalog no. 30-0035) purchased from Harvard Apparatus (Holliston, MA) (48). Immediately prior to analysis, samples were desalted from their incubation buffer into 100 mM ammonium acetate using a HiTrap desalting column from GE Healthcare. The *m/z* scale on the quadrupole TOF was calibrated from 500–8,000 using perfluoroheptanoic acid. CCS values were estimated from a calibration curve of native-like proteins using calibrants and methods that were described previously (49). Data analysis was carried out using Waters MassLynx 4.1. Theoretical CCS values were calculated using Waters Driftscope.

Transmission electron microscopy (TEM)

TEM images were obtained on a JEOL2000FX transmission electron microscope. Prior to imaging, incubated samples were spun at 14,000 rpm for 45 min. The supernatant was then removed, and the pellet was resuspended with 10 μl of deionized water. The samples were applied dropwise to 300-mesh carbon-coated copper grids (catalog no. CF300-CU) obtained from Electron Microscopy Services and allowed to dry. The samples were then stained with a 1% (w/v) solution of phosphotungstic acid adjusted to pH 7.4 with potassium hydroxide. Following a water rinse, the samples were dried overnight and protected from ambient light until analysis.

Fluorescence spectroscopy

To measure the binding affinity of Cu(II) to β2m, a PTI Quantamaster 300 was used. Intrinsic fluorescence was monitored via excitation at 295 nm, whereas emission was monitored from 300–400 nm. Prior to measurement, the samples were equilibrated at ambient room temperature for 15 min. The fraction bound was determined by measuring the average emission intensity ($<\lambda>$) via intrinsic Trp fluorescence. Cu(II) concentrations were refined using the Hyperquad Simulation and Speciation (HySS) software (Protonic Software). Solution conditions for the affinity measurements were carried out using similar solution conditions as those described above. Data were plotted using Origin (Northampton, MA), and the titration data were fitted using the Hill equation.

Author contributions—T. M. M. conducted most of the experiments, analyzed the results, and wrote most of the paper. J. D., R. L., and K. V. D. conducted some of the SEC experiments and studied the dissolution of β2m aggregates by SDS. R. W. V. conceived the idea for the project and wrote the paper with T. M. M.

Acknowledgments—We acknowledge Dr. Steve Eyles of the University of Massachusetts Mass Spectrometry Center for assistance with instrumentation. We also thank Louis Raboin of the University of Massachusetts Electron Microscopy Center for assistance with sample preparation and imaging. We also acknowledge Dr. Eugenia Clerico for help with preparing nanospray tips.

References

1. Doig, A. J., and Derreumaux, P. (2015) Inhibition of protein aggregation and amyloid formation by small molecules. *Curr. Opin. Struct. Biol.* **30,** 50–56
2. Cheng, B., Gong, H., Xiao, H., Petersen, R. B., Zheng, L., and Huang, K. (2013) Inhibiting toxic aggregation of amyloidogenic proteins: a therapeutic strategy for protein misfolding diseases. *Biochim. Biophys. Acta* **1830,** 4860–4871
3. Drüeke, T. B., and Massy, Z. A. (2009) β2-microglobulin. *Semin. Dial.* **22,** 378–380
4. Gejyo, F., Odani, S., Yamada, T., Honma, N., Saito, H., Suzuki, Y., Nakagawa, Y., Kobayashi, H., Maruyama, Y., and Hirasawa, Y. (1986) β_2-microglobulin: a new form of amyloid protein associated with chronic hemodialysis. *Kidney Int.* **30,** 385–390
5. Katou, H., Kanno, T., Hoshino, M., Hagihara, Y., Tanaka, H., Kawai, T., Hasegawa, K., Naiki, H., and Goto, Y. (2002) The role of the disulfide bond in the amyloidogenic state of β_2-microglobulin studied by heteronuclear NMR. *Protein Sci.* **11,** 2218–2229
6. Danesh, F., and Ho, L. T. (2001) Dialysis-related amyloidosis: history and clinical manifestations. *Semin. Dial.* **14,** 80–85
7. McParland, V. J., Kad, N. M., Kalverda, A. P., Brown, A., Kirwin-Jones, P., Hunter, M. G., Sunde, M., and Radford, S. E. (2000) Partially unfolded states of β_2-microglobulin and amyloid formation *in vitro*. *Biochemistry* **39,** 8735–8746
8. Rennella, E., Corazza, A., Giorgetti, S., Fogolari, F., Viglino, P., Porcari, R., Verga, L., Stoppini, M., Bellotti, V., and Esposito, G. (2010) Folding and fibrillogenesis: clues from β-2-microglobulin. *J. Mol. Biol.* **401,** 286–297
9. Sasahara, K., Yagi, H., Naiki, H., and Goto, Y. (2007) Heat-induced conversion of β2-microgloublin and hen egg-white lysozyme into amyloid fibrils. *J. Mol. Biol.* **372,** 981–991
10. Ookoshi, T., Hasegawa, K., Ohhashi, Y., Kimura, H., Takahashi, N., Yoshida, H., Miyazaki, R., Goto, Y., and Naiki, H. (2008) Lysophospholipids induce the nucleation and extension of β2-microglobulin related amyloid fibrils at a neutral pH. *Nephrol. Dial. Transplant.* **23,** 3247–3255
11. Eichner, T., and Radford, S. E. (2011) Understanding the complex mechanisms of β_2-microglobulin amyloid assembly. *FEBS J.* **278,** 3868–3883
12. Morgan, C. J., Gelfand, M., Atreya, C., and Miranker, A. D. (2001) Kidney dialysis-associated amyloidosis: a molecular role for copper in fiber formation. *J. Mol. Biol.* **309,** 339–345
13. Eakin, C. M., Knight, J. D., Morgan, C. J., Gelfand, M. A., and Miranker, A. D. (2002) Formation of a copper specific binding site in non-native states of β-2-microglobulin. *Biochemistry* **41,** 10646–10656
14. Eakin, C. M., Attenello, F. J., Morgan, C. J., and Miranker, A. D. (2004) Oligomeric assembly of native-like precursors precedes amyloid formation by β-2 microglobulin. *Biochemistry* **43,** 7808–7815
15. Antwi, K., Mahar, M., Srikanth, R., Olbris, M. R., Tyson, J. F., and Vachet, R. W. (2008) Cu(II) organizes β-2-microglobulin oligomers but is released upon amyloid formation. *Protein Sci.* **17,** 748–759
16. Dong, J., Joseph, C. A., Borotto, N. B., Gill, V. L., Maroney, M. J., and Vachet, R. W. (2014) Unique effect of Cu(II) in the Metal-induced amyloid formation of β-2-microglobulin. *Biochemistry* **53,** 1263–1274
17. Mendoza, V. L., Antwi, K., Barón-Rodríguez, M. A., Blanco, C., and Vachet, R. W. (2010) Structure of the preamyloid dimer of β-2-microglobulin from covalent labeling and mass spectrometry. *Biochemistry* **49,** 1522–1532
18. Mendoza, V. L., Barón-Rodríguez, M. A., Blanco, C., and Vachet, R. W. (2011) Structural insights into the pre-amyloid tetramer of β-2-microglobulin from covalent labeling and mass spectrometry. *Biochemistry* **50,** 6711–6722
19. Srikanth, R., Mendoza, V. L., Bridgewater, J. D., Zhang, G., and Vachet, R. W. (2009) Copper binding to β-2-microglobulin and its pre-amyloid oligomers. *Biochemistry* **48,** 9871–9881
20. Lim, J., and Vachet, R. W. (2004) Using mass spectrometry to study copper-protein binding under native and non-native conditions: β-2-microglobulin. *Anal. Chem.* **76,** 3498–3504
21. Quaglia, M., Carazzone, C., Sabella, S., Colombo, R., Giorgetti, S., Bellotti, V., and De Lorenzi, E. (2005) Search of ligands for the amyloidogenic protein β_2-microglobulin by capillary electrophoresis and other techniques. *Electrophoresis* **26,** 4055–4063
22. Regazzoni, L., Colombo, R., Bertoletti, L., Vistoli, G., Aldini, G., Serra, M., Carini, M., Facino, R. M., Giorgetti, S., Stoppini, M., Caccialanza, G., and De Lorenzi, E. (2011) Screening of fibrillogenesis inhibitors of β_2-microglobulin: integrated strategies by mass spectrometry capillary electrophoresis and *in silico* simulations. *Anal. Chim. Acta* **685,** 153–161
23. Woods, L. A., Platt, G. W., Hellewell, A. L., Hewitt, E. W., Homans, S. W., Ashcroft, A. E., and Radford, S. E. (2011) Ligand binding to distinct states diverts aggregation of an amyloid-forming protein. *Nat. Chem. Biol.* **7,** 730–739
24. Giorgetti, S., Raimondi, S., Pagano, K., Relini, A., Bucciantini, M., Corazza, A., Fogolari, F., Codutti, L., Salmona, M., Mangione, P., Colombo, L., De Luigi, A., Porcari, R., Gliozzi, A., Stefani, M., *et al.* (2011) Effect of tetracyclines on the dynamics of formation and destructuration of β2-microglobulin amyloid fibrils. *J. Biol. Chem.* **286,** 2121–2131
25. Carazzone, C., Colombo, R., Quaglia, M., Mangione, P., Raimondi, S., Giorgetti, S., Caccialanza, G., Bellotti, V., and De Lorenzi, E. (2008) Sulfonated molecules that bind a partially structured species of β2-microglobulin also influence refolding and fibrillogenesis. *Electrophoresis* **29,** 1502–1510

26. Meng, F., Marek, P., Potter, K. J., Verchere, C. B., and Raleigh, D. P. (2008) Rifampicin does not prevent amyloid fibril formation by human islet amyloid polypeptide but does inhibit fibril thioflavin-T interactions: implications for mechanistic studies of β-cell death. *Biochemistry* **47,** 6016–6024
27. Woods, L. A., Radford, S. E., and Ashcroft, A. E. (2013) Advances in ion mobility spectrometry-mass spectrometry reveal key insights into amyloid assembly. *Biochim. Biophys. Acta.* **1834,** 1257–1268
28. Williams, D. M., and Pukala, T. L. (2013) Novel insights into protein misfolding diseases revealed by ion mobility-mass spectrometry. *Mass Spectrom. Rev.* **32,** 169–187
29. Beveridge, R., Chappuis, Q., Macphee, C., and Barran, P. (2013) Mass spectrometry methods for intrinsically disordered proteins. *Analyst* **138,** 32–42
30. Lanucara, F., Holman, S. W., Gray, C. J., and Eyers, C. E. (2014) The power of ion mobility-mass spectrometry for structural characterization and the study of conformational dynamics. *Nat. Chem.* **6,** 281–294
31. Hyung, S. J., and Ruotolo, B. T. (2012) Integrating mass spectrometry of intact protein complexes into structural proteomics. *Proteomics* **12,** 1547–1564
32. Ruotolo, B. T., Benesch, J. L., Sandercock, A. M., Hyung, S. J., and Robinson, C. V. (2008) Ion mobility-mass spectrometry analysis of large protein complexes. *Nat. Protoc.* **3,** 1139–1152
33. Ruotolo, B. T., Giles, K., Campuzano, I., Sandercock, A. M., Bateman, R. H., and Robinson, C. V. (2005) Evidence for macromolecular protein rings in the absence of bulk water. *Science* **310,** 1658–1661
34. Scarff, C. A., Patel, V. J., Thalassinos, K., and Scrivens, J. H. (2009) Probing hemoglobin structure by means of traveling-wave ion mobility mass spectrometry. *J. Am. Soc. Mass Spectrom.* **20,** 625–631
35. Seo, J., Hoffmann, W., Warnke, S., Bowers, M. T., Pagel, K., and von Helden, G. (2016) Retention of native protein structures in the absence of solvent: a coupled ion mobility and spectroscopic study. *Angew. Chem. Int. Ed. Engl.* **55,** 14173–14176
36. Sun, Y., Vahidi, S., Sowole, M. A., and Konermann, L. (2016) Protein structural studies by traveling wave ion mobility spectrometry: a critical look at electrospray sources and calibration issues. *J. Am. Soc. Mass Spectrom.* **27,** 31–40
37. Maurer, M. M., Donohoe, G. C., and Valentine, S. J. (2015) Advances in ion mobility-mass spectrometry instrumentation and techniques for characterizing structural heterogeneity. *Analyst* **140,** 6782–6798
38. Jezowska-Bojczuk, M., Lambs, L., Kozlowski, H., and Berthon, G. (1993) Metal ion-tetracycline interactions in biological fluids. 10. Structural investigation on copper (II) complexes of tetracycline, oxytetracycline, chlortetracycline, 4-(dedimethylamino)tetracycline, and 6-desoxy-6-demthyltetracycline and discussion of their binding modes. *Inorg. Chem.* **32,** 428–437
39. Brion, M., Lambs, L., and Berthon, G. (1986) Metal ion-tetracycline interactions in biological fluids. Part 6. Formation of copper(II) complexes with tetracycline and some of its derivatives and appraisal of their biological significance. *Inorg. Chim. Acta* **123,** 61–68
40. Bleiholder, C., Do, T. D., Wu, C., Economou, N. J., Bernstein, S. S., Buratto, S. K., Shea, J. E., and Bowers, M. T. (2013) Ion mobility spectrometry reveals the mechanism of amyloid formation of Aβ(25–35) and its modulation by inhibitors at the molecular level: epigallocatechin gallate and *scyllo*-inositol. *J. Am. Chem. Soc.* **135,** 16926–16937
41. Liang, Y., Ore, M. O., Morin, S., and Wilson, D. J. (2012) Specific disruption of transthyretin(105–115) Fibrillization using "stabilizing" inhibitors of transthyretin amyloidogenesis. *Biochemistry* **51,** 3523–3530
42. Soto-Ortega, D. D., Murphy, B. P., Gonzalez-Velasquez, F. J., Wilson, K. A., Xie, F., Wang, Q., and Moss, M. A. (2011) Inhibition of amyloid-β aggregation by coumarin analogs can be manipulated by functionalization at the aromatic center. *Bioorg. Med. Chem.* **19,** 2596–2602
43. Sengupta, U., Nilson, A. N., and Kayed, R. (2016) The role of amyloid-β oligomers in toxicity, propagation, and immunotherapy. *EBioMedicine* 10.1016/j.ebiom.2016.03.035
44. Cerasoli, E., Ryadnov, M. G., and Austen, B. M. (2015) The elusive nature and diagnostics of misfolded Aβ oligomers. *Front. Chem.* 10.3389/fchem.2015.00017
45. Marshall, K. E., Marchante, R., Xue, W. F., and Serpell, L. C. (2014) The relationship between amyloid structure and cytotoxicity. *Prion* 10.4161/pri.28860
46. Fändrich, M. (2012) Oligomeric intermediates in amyloid formation: structure determination and mechanisms of toxicity. *J. Mol. Biol.* **421,** 427–440
47. Larson, M. E., and Lesné, S. E. (2012) Soluble Aβ oligomer production and toxicity. *J. Neurochem.* **120,** 125–139
48. Hernández, H., and Robinson, C. V. (2007) Determining the stoichiometry and interactions of macromolecular assemblies from mass spectrometry. *Nat. Protoc.* **2,** 715–726
49. Bush, M. F., Hall, Z., Giles, K., Hoyes, J., Robinson, C. V., and Ruotolo, B. T. (2010) Collision cross sections of proteins and their complexes: a calibration framework and database for gas-phase structural biology. *Anal. Chem.* **15,** 9557–9565